for precise evaluation of the linewidth when the surface is prepared with the 500-grit size wheel.

No allowance was made for the possibility of demagnetizing the higher peaks of the surface. These peaks would be observed optically but the reduced magnetization in these peaks would appear as a magnetic smoothing of the surface. We therefore expect the observed linewidth to be less than predicted. The only reason to expect an increase of the ferromagnetic linewidth over the prediction would be the possibility that spectral contributions which contribute to the linewidth were masked by the spectral density which was observed.

The predicted and observed linewidth for spheres prepared with the 500-grit size wheel are given in Table III. The agreement is poor, as is anticipated from theoretical considerations.

The observations of linewidth for one additional sphere are not reported here. These linewidths could not be interpreted within the scope of the theory presented here. A degenerate resonant mode[11] was strongly coupled to the uniform precession mode in the range of frequencies over which the linewidths were observed. The experimental evidence for the degenerate mode was the occurrence of a double-resonance mode and a strong dependence of apparent linewidth on frequency.

ACKNOWLEDGMENTS

I would like to thank J. O. Artman of the Carnegie Institute of Technology and N. Karayianis of this Laboratory for their continuing interest and encouragement throughout the research and the preparation of this manuscript. In addition, I would like to express gratitude to the following: L. Joseph of the National Bureau of Standards for providing the computation of the integral required on the linewidth calculation, O. Cruzan of the Harry Diamond Laboratories for programming the interference microscope data, and to J. R. Cuthill of the National Bureau of Standards for the use of the interference microscope.

[11] L. R. Walker, Phys. Rev. **105**, 390 (1957).

PHYSICAL REVIEW VOLUME 137, NUMBER 1A 4 JANUARY 1965

Spectroscopy of MnO_4^{3-} in Calcium Halophosphates

J. D. KINGSLEY, J. S. PRENER, AND B. SEGALL
General Electric Research Laboratory, Schenectady, New York

(Received 28 July 1964)

A study has been made of the optical absorption and fluorescence of the compounds Ca_2PO_4Cl (spodiosite) and $Ca_5(PO_4)_3Cl$ (apatite) doped with Mn^{5+}. The Mn^{5+} ion has the electronic configuration $3d^2$ and it substitutes for the phosphorous ion, producing the hypomanganate ion, MnO_4^{3-}. The Mn^{5+} ion is in a field with a symmetry that is approximately tetrahedral (T_d) but the lower symmetry components are strong enough to split the energy levels by several hundred cm^{-1}. The prominent features of the absorption spectra are two sharp lines between 8300 and 8800 cm^{-1}, two strong broad bands between 12 000 and 20 000 cm^{-1}, a third strong band near 31 000 cm^{-1}, and a complex structure between 21 000 and 25 000 cm^{-1}. We believe that the sharp lines are due to transitions ($^3A_2 \rightarrow {}^1E$) within the ground-state (e^2) configuration, while the three strong bands (oscillator strengths from 3×10^{-3} to 3×10^{-2}) are due to the three lowest-energy allowed one-electron transitions, $e^2:{}^3A_2 \rightarrow et_2:{}^3T_1$, $e^2:{}^3A_2 \rightarrow t_1{}^5e^3:{}^3T_1$, and $e^2:{}^3A_2 \rightarrow t_1{}^5e^2t_2:{}^3T_1$, the t_1 orbitals consisting entirely of ligand (oxygen) orbitals. We deduce a value of 11 000 cm^{-1} for the ligand field-strength parameter Δ, and a value of 550 cm^{-1} for the Racah parameter B. Radiation absorbed in the strong bands produces fluorescence at the same energies as the infrared absorption lines. These lines are accompanied by weak satellite-emission lines and bands that occur because various vibrations of the MnO_4^{3-} ion and the host lattice can be excited simultaneously with the electronic transition. The complex, structured absorption between 21 000 and 25 000 cm^{-1} is a manifestation of other vibronic transitions. We have deduced an energy of 750 cm^{-1} for the A_1 vibrational mode and 245 cm^{-1} for the E mode. The lattice vibrational spectrum of Ca_2PO_4Cl has 15 cm^{-1} as a characteristic frequency.

INTRODUCTION

THE optical absorption of the MnO_4^{-3} ion in strongly alkaline aqueous solutions has been reported,[1–3] and attempts have been made to interpret the spectra in terms of proposed electronic structures.[4–6] No data have been available on the optical properties of this ion in a solid, however. One might expect that the spectra of this ion in a solid would exhibit more detail which would allow one to obtain more definite in-

[1] A. Carrington and M. C. R. Symons, J. Chem. Soc. **1956**, 3373 (1956).
[2] A. Carrington, D. J. E. Ingram, D. S. Schonland, and M. C. R. Symons, J. Chem. Soc. **1956**, 4710 (1956).
[3] C. Furlani, A. Ciana, and G. Batticci, Univer. Trieste, Fac. Sci. Ist. Chim., Studi **25** (1958).
[4] M. Wolfsberg and L. Helmholtz, J. Chem. Phys. **20**, 837 (1952).
[5] C. J. Ballhausen and A. D. Liehr, J. Mol. Spectry. **2**, 342 (1958).
[6] A. Carrington and D. S. Schonland, Mol. Phys. **3**, 331 (1960).

formation about the electronic structure. This indeed has proved to be the case.

During the course of our work on the growth of calcium halophosphate crystals, we found it possible to incorporate Mn as MnO_4^{3-} at PO_4^{3-} sites. Studies of the optical transmission of some of these crystals revealed that in addition to the broad absorption bands (which upon close examination are in fact found to reveal structure) similar to those observed previously in solution, there were weak narrow absorption lines in the infrared and visible regions of the spectrum. Furthermore, excitation into the broad visible absorption bands resulted in intense narrow-line infrared fluorescence, an observation unique for a transition metal with a d^2 configuration. Finally in both the infrared fluorescence and the weak absorption bands in the visible, a large number of unusually well-resolved satellites are observed, which are due to phonon absorption and emission accompanying the electronic transitions.

In this paper we briefly discuss the preparation of the crystals, and give a description of the rather rich absorption and emission spectra that have been observed. We interpret the spectra in terms of the electronic states of the MnO_4^{3-} complex and the vibrational modes of the complex and host to which the electronic states are coupled.

CRYSTAL GROWTH

The phase diagrams for the binary systems $Ca_3(PO_4)_2$-$CaCl_2$ and $Ca_3(PO_4)_2$-CaF_2 as well as part of the ternary system were determined by Nacken.[7] In the chloride system two solid phases were found: Ca_2PO_4Cl similar to the mineral spodiosite and $Ca_5(PO_4)_3Cl$ with the apatite structure. The former melts incongruently at 1040°C, whereas the latter melts at temperatures in excess of 1600°C. The fluoride system contains but one compound $Ca_5(PO_4)_3F$, which has the apatite structure and melts at about 1650°C.

Large single crystals of $Ca_5(PO_4)_3F$ have been grown using the Kyropoulus method.[8] Because of the rapid vaporization of $CaCl_2$ at the high temperatures, $Ca_5(PO_4)_3Cl$ could not be grown by this method. Spodiosite Ca_2PO_4Cl cannot, of course, be grown from a melt of the same composition due to its incongruent melting point. Small crystals of both chloride compounds (1 to 3 mm in size) suitable for optical studies have been grown from a saturated solution of the compounds in fused $CaCl_2$ by slow cooling. Larger crystals (5 to 10 mm) of spodiosite have been grown by the thermal gradient method,[9] again from fused $CaCl_2$ as a solvent.

TABLE I. Chemical analysis of calcium chlorophosphates.

	% Cl		% Ca		% PO_4	
	Found	Calc	Found	Calc	Found	Calc
Spodiosite Ca_2PO_4Cl	16.7±0.1	16.8	38.2±0.1	38.1	44.9±0.2	45.1
Apatite $Ca_5(PO_4)_3Cl$	6.7±0.1	6.8	38.5±0.1	38.5	54.2±0.2	54.7

Typical melt compositions were:

	wt $CaCl_2$	wt $Ca_5(PO_4)_3Cl$	Liquidus Temp.
Spodiosite Ca_2PO_4Cl	40.0 g	5.1 g	990°C
Apatite $Ca_5(PO_4)_3Cl$	30.0 g	11.7 g	1230°C.

The $Ca_5(PO_4)_3Cl$ was obtained from the Chemical Products Plant of the General Electric Company.

The melts were kept in covered platinum crucibles at temperatures some 50°C above the reported liquidus temperature for 24 h and were then cooled at linear rates varying between 2 to 5°C per hour until a temperature of about 800°C was reached for spodiosite or 1050°C for apatite. The furnace power was then shut off and the crucibles cooled rapidly to room temperature. The crystals of both calcium halophosphates could be separated readily from the $CaCl_2$ by leaching with hot water. The unit cell dimensions of the orthorhombic Ca_2PO_4Cl as determined from single crystal x ray diffraction photographs were $a=6.18$ Å, $b=6.98$ Å, and $c=10.81$ Å; the volume of the unit cell is 4.68×10^{-22} cm^3 and contains, therefore, four "molecules" of Ca_2PO_4Cl using the density of 3.00 g/cm^3.[10] The optical transmission of both spodiosite and chlorapatite have been determined. Both of these compounds are transmitting up to about 7.5 eV but appear to have impurity or defect absorption at lower energies. The results of the chemical analysis of the crystals given in Table I indicate that the crystals as grown are of stoichiometric composition.

In addition to these two phases, we have also grown mixed fluor-chlorapatite crystals from a mixed $CaCl_2$-CaF_2 melt.

For the thermal gradient growth of spodiosite the charge consisted of 150 g of $CaCl_2$ and 18 g of $Ca_5(PO_4)_3Cl$ contained in a platinum crucible. A temperature of 834°C was established at the top of the liquid phase and 849°C at the bottom of the charge. A small seed crystal of spodiosite was immersed in the liquid at the top to a depth of about 0.5 mm, rotated and withdrawn at a rate of about 1 to 2 mm per day. The c axis of the crystal was parallel to the rotation axis. A large crystal (0.5 to 1 cm) grew on the seed in three days. Large spodiosite crystals containing MnO_4^{-3} were also grown by this method.

MANGANESE-DOPED CRYSTALS

When in addition to the required amounts of $CaCl_2$, CaF_2, and $Ca_5(PO_4)_3Cl$, about 0.03 to 0.05% by weight of anhydrous $MnCl_2$ was added to the charge, and

[7] R. Nacken, Centr. Min. Geol. **1912**, 545 (1912).
[8] P. D. Johnson, J. Electrochem. Soc. **108**, 159 (1960).
[9] G. F. Reynolds and H. J. Guggenheim, J. Phys. Chem. **65**, 1655 (1961).
[10] G. A. Jeffrey and S. C. Chang, (private communication).

crystal growth took place in an atmosphere containing some oxygen, the resulting spodiosite and apatite crystals were colored deep blue. Several of the different crystalline products were analyzed colorimetrically for total Mn by oxidation to permanganate,[11] and for manganese in an oxidation state higher than two using As_2O_3 in dilute sulfuric acid as the reducing agent.[12] The results of a number of products are summarized in Table II.

The fact that the calculated average valence of the manganese was close to +5 independent of the amount of manganese, the solid phase and the atmosphere in which the crystals were grown suggests that the manganese is present in the +5 state. From these results and the fact that Mn could not be detected in spodiosite grown in an argon atmosphere, indicates that Mn^{+2} is rejected during crystal growth. Preliminary electron-spin-resonance measurements by Ludwig on the spodiosite crystals containing manganese indicated the presence of manganese in a state other than Mn^{2+} and only a very small amount of Mn^{2+}.

Because of its high charge state, it seems unlikely that Mn^{5+} could exist in these compounds except at a substitutional site. Furthermore, it is much more likely that this is a phosphorous site than a calcium site. The valency determination thus implies that the manganese exists as a MnO_4^{3-} ion substituting for a PO_4^{3-} ion. Lux[13] reported isomorphous substitution of PO_4^{3-} and VO_4^{3-} by MnO_4^{3-}, and Klemm[14] prepared polycrystalline $Ba_3(MnO_4)_2$ and $Ba_5(MnO_4)_3OH$ which gave the same x ray diffraction patterns as $Ba_3(PO_4)_2$ and the apatite $Ba_5(PO_4)_3OH$, respectively. These observations support our hypothesis concerning the Mn^{5+} site.

TABLE II. Average valence of Mn in halophosphate crystals.

	Total Mn % by wt	Calc average valence	Atmosphere during growth
Ca_2PO_4Cl	0.028	+5.2±0.2	Air
Ca_2PO_4Cl	0.061	+5.0±0.2	Oxygen
Ca_2PO_4Cl	0.025	+5.5±0.2	Argon-Oxygen (10:1)
Ca_2PO_4Cl	<0.005	···	Argon
$Ca_5(PO_4)_3Cl$	0.0033	+5.0±0.2	Air
$Ca_5(PO_4)_3Cl$	0.031	+5.0±0.2	Air

OPTICAL ABSORPTION

The optical absorption of the halophosphate crystals was measured using a Cary Model 14 spectrophotometer and a Jarrell-Ash 0.5-m monchromator. Low temperature absorption data were obtained with a Hofman double vessel stainless steel cryostat. Because of our lack of knowledge of the spodiosite site symmetry and the smallness of our apatite crystals, we were not able to advantageously utilize polarized radiation. Unless stated otherwise, unpolarized radiation was used in taking the data presented here. The absorption coefficient of the undoped crystals was less than 5 cm^{-1} for wavelengths longer than 2500 Å. The observed absorption is summarized in Table III and is described and interpreted below.

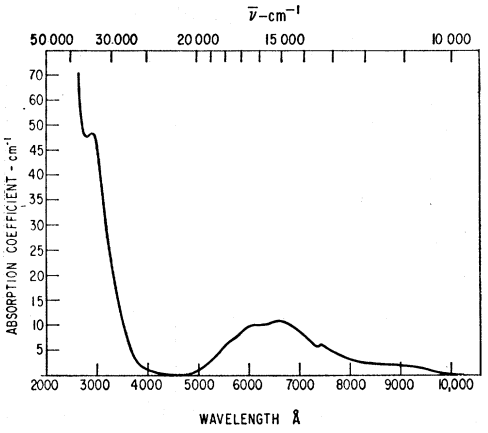

FIG. 1. Optical absorption spectrum at room temperature of $Ca_5(PO_4)_3Cl$ containing 1.1×10^{19} manganese/cm^3.

A. Broad Absorption Bands

The room temperature absorption of manganese-doped chlorapatite is shown in Fig. 1, and Fig. 2 shows the absorbance of a dilute solution of MnO_4^{-3} in 12*M* aqueous NaOH solution prepared by the method of

TABLE III. Electronic absorption spectra of MnO_4^{-3} in halophosphates. (bb: broad bands; brb: barely resolved band; nwb: narrow weak band; bwb: broad weak band; sl: sharp lines.)

Excited electronic state Ground state $^3A_2(t_1^6e^2)$	Observed energies (cm^{-1}) $Ca_5(PO_4)_3Cl$ (Apatite)	Ca_2PO_4Cl (Spodiosite)
$^3T_1(t_1^5e^2t_2)$	33 500 bb	32 400 bb
$^1T_2(t_1^6et_2)$	···[a]	25 000–21 500[b]
$^3T_1(t_1^6et_2)$ } [c]	16 700 brb	17 500[d] bb
$^3T_1(t_1^5e^3)$ }	14 800 bb	13 800[d] bb
$^1A_1(t_1^6e^2)$	13 600 nwb	···
$^3T_2(t_1^6et_2)$	11 000 bwb	11 000 bwb
$^1E(t_1^6e^2)$	8764, 8598[e] sl	8703, 8410[e] sl

[a] Only very weak (<0.1 cm^{-1} absorption coefficient) absorption observed exhibiting structureless oscillations of the absorption coefficient with a period of ~900 cm^{-1}.

[b] Complex spectrum consisting of five components uniformly spaced at 750 cm^{-1}. Each component exhibits a complex structure (see text). Spectrum arises from excitation of electronic transitions in MnO_4^{-3} ion combined with excitation or de-excitation of localized and lattice vibrations.

[c] Specific assignment of observed bands to particular transitions cannot be made.

[d] The 17 500 band at 2°K exhibits structure with maxima 17 600, 17 920, and 18 330 cm^{-1}. The 13 800 cm^{-1} band has maxima at 12 740, 13 100, and 13 790 cm^{-1}. These arise from the removal of the orbital degeneracy of the $^3T_1$ excited state by lower symmetry components of the crystal field.

[e] The two lines result from removing the orbital degeneracy of the excited ^1E state by lower symmetry components of the crystal field. These lines are seen in both emission and absorption in $Ca_2PO_4Cl:MnO_4^{-3}$.

[11] E. B. Sandell, *Colorimetric Determination of Traces of Metals* (Interscience Publishers, Inc., New York, 1959), p. 608.

[12] I. M. Kolthoff and E. B. Sandell, *Textbook of Quantitative Inorganic Analysis* (The Macmillan Company, New York, 1947), p. 605.

[13] H. Lux, Z. Naturforsch. **1**, 281 (1946).

[14] W. Klemm, *International Symposium on the Reactivity of Solids* (1952), p. 173.

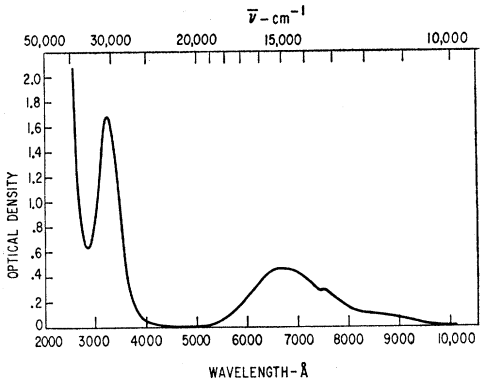

FIG. 2. Optical absorption spectrum at room temperature of an aqueous solution of MnO_4^{-3} in 12M NaOH.

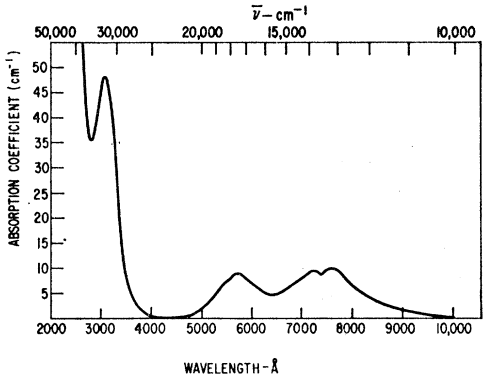

FIG. 3. Optical absorption spectrum at room temperature of Ca_2PO_4Cl containing 9.8×10^{18} manganese/cm^3.

Lux.[13] There is a strong similarity between the spectra of Figs. 1 and 2, which again indicates that the manganese in the solid is present as the MnO_4^{3-} ion. The absorption spectrum of a mixed fluor-chlorapatite containing Mn is very similar to that of the chlorapatite.

In Fig. 3. we show the absorption of a sample of manganese-doped spodiosite crystal, and again a similarity with the MnO_4^{3-} spectrum can be seen. In this case, however, the broad band which is at 14 800 cm^{-1} in the liquid solution splits into bands at 17 500 and 13 800 cm^{-1}. The bands in the visible exhibit a structure which will be considered below.

B. Line Absorption

The absorption of a manganese-doped spodiosite crystal (1.1×10^{19} Mn per cm^3) at 2°K is shown in Fig. 4 The broad bands noted above are seen to be somewhat narrower than at room temperature and various sharp lines can be seen at 8410, 8703, and between 21 500 and 25 000 cm^{-1}.

The spectrum between 21 500 and 25 000 cm^{-1} consists of five components uniformly spaced at 750 cm^{-1}. The second of these (in terms of increasing frequency) is strongest and the amplitudes of the higher components decrease in size monatonically. Figure 5 shows the two lowest energy, and strongest, components. Each component consists of a strong pair of lines about 20 cm^{-1} apart, a weaker pair of lines 460 cm^{-1} higher in energy, and a continuum absorption which extends from the strong lines out to 390 cm^{-1} from them.

The weaker parts of this spectrum are shown in better detail in Fig. 6, taken on a crystal at 2°K, indicating that superposed on the continuum are five narrow bands (about 20 cm^{-1} wide) located 60, 90, 120, 150, and 180 cm^{-1} from the stronger line. At temperatures above 20°K a continuum on the low-energy side of the strong lines can be discerned. This continuum becomes stronger and the lines become broader and weaker with increasing temperature.

We interpret this spectrum as arising from the optical

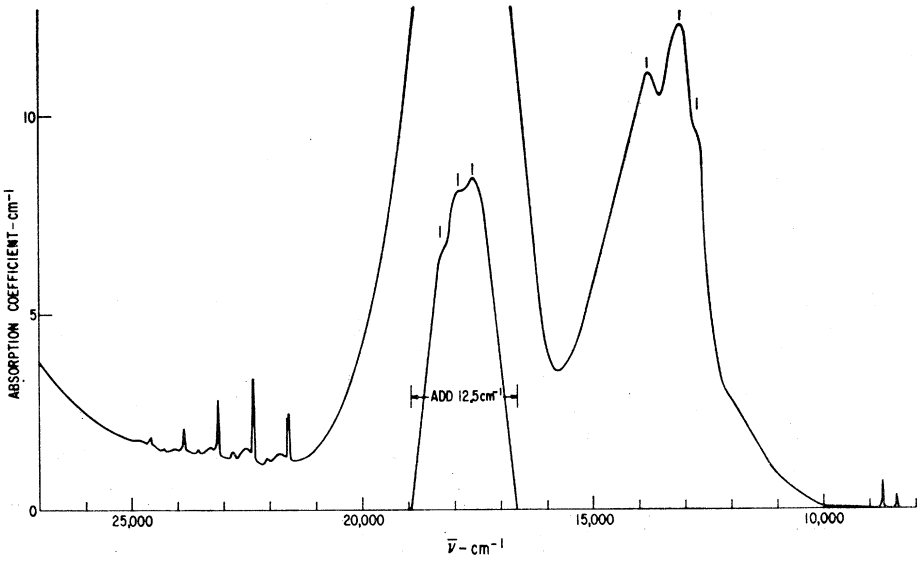

FIG. 4. Optical absorption spectrum at 2°K of Ca_2PO_4Cl containing 1.1×10^{19} manganese/cm^3. Incident radiation polarized with **E** parallel to b axis of unit cell.

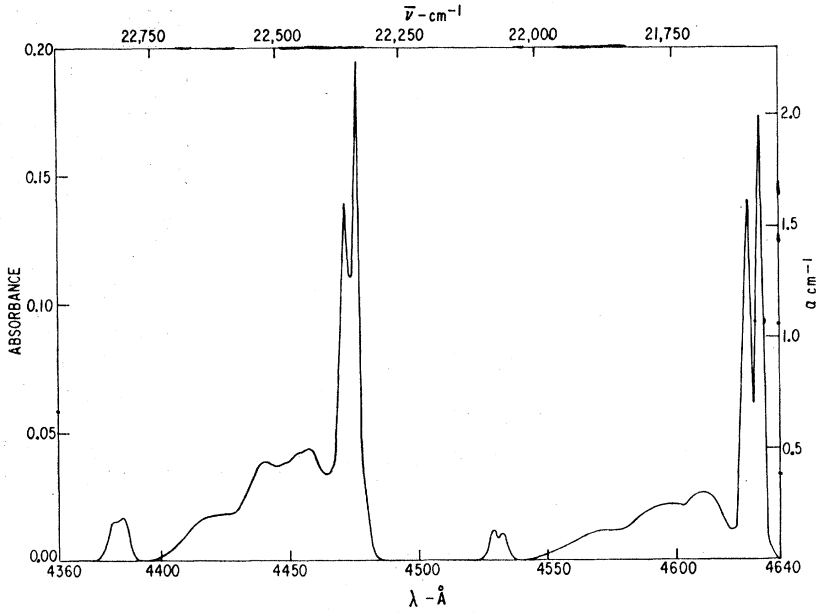

FIG. 5. Optical absorption spectrum at 10°K of Ca_2PO_4Cl containing 1.1×10^{19} manganese/cm^3.

excitation of electronic transitions of the MnO_4^{3-} ion combined with the excitation or de-excitation of one or more vibrations of the MnO_4^{3-} ion and the lattice. Our assignment of these vibrations will be described in the Discussion.

Excitations similar to these could not be found in the manganese-containing apatite crystals. There were only structureless oscillations in the absorption coefficient with a period of approximately 900 cm^{-1} and magnitudes less than 0.1 cm^{-1}.

The absorption lines in spodiosite in the infrared do not show any structure such as that seen in the blue. Our instrumental sensitivity was such that we could have seen phonon-assisted transitions 5% as intense as the line at 8703 cm^{-1}. Absorption measurements using the Jarrell-Ash monochromator indicated that the line at 8410 cm^{-1} has a width of about 1 cm^{-1} at 4°K.

The oscillator strength of the 8410 cm^{-1} line is about 6.5×10^{-7} and that of the 8703 cm^{-1} line is about 1.6×10^{-6} or a ratio of 2:5. These are of the order of magnitude of the strengths of spin-forbidden intraconfigurational transitions. The ratio of the line

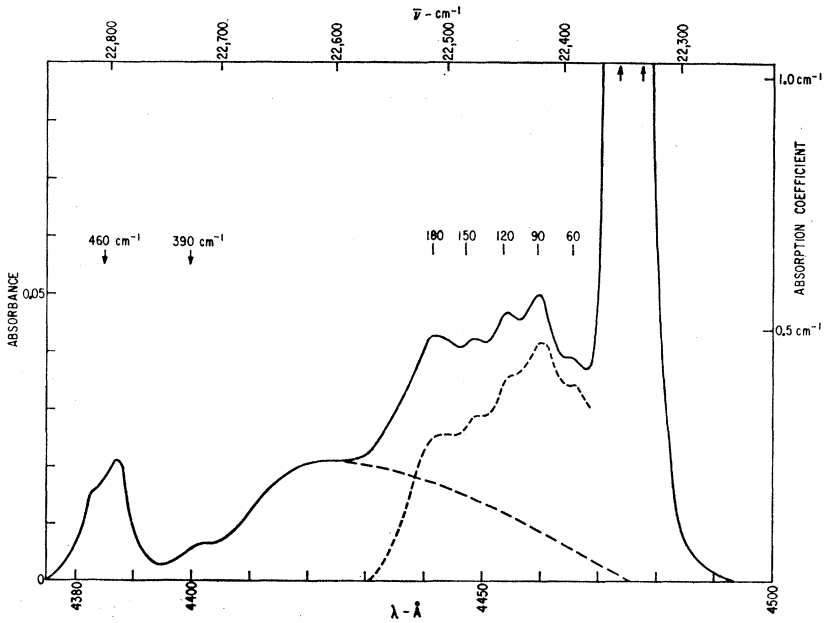

FIG. 6. Optical absorption spectrum at 2°K of Ca_2PO_4Cl containing 1.1×10^{19} manganese/cm^3.

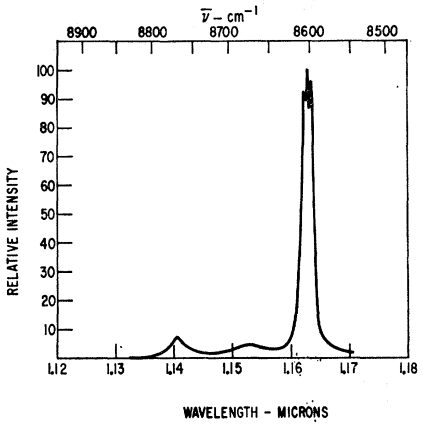

FIG. 7. Emission spectrum of $Ca_5(PO_4)_3Cl:MnO_4^{3-}$ at 78°K. The same spectra are observed for manganese concentrations of 1.1×10^{19} and 1.2×10^{18} cm^{-3}.

strengths was measured at temperatures up to 78°K and no strong dependence on temperature was found indicating that both lines originate from the same state.

INFRARED FLUORESCENCE

All of the blue crystals fluoresce in the infrared when excited with visible radiation. The fluorescence spectra taken at 78°K of chlorapatite and fluorapatite containing Mn are shown in Figs. 7 and 8. The emission spectrum of mixed fluor-chlorapatite crystals containing Mn is similar to those shown. Figure 9 shows the emission spectrum of spodiosite. The excitation for these spectra was obtained from an incandescent lamp filtered by a Corning C.S. 4-94 filter. The spectra were measured with the Jarrell-Ash monochromator and a 7102 photomultiplier. No correction for the wavelength dependence of the detector sensitivity has been made. A simultaneous measurement of the line absorption and emission in $Ca_2PO_4Cl:MnO_4^{3-}$ indicated no Stoke's shift larger than a fraction of the linewidth.

It can be seen from Fig. 9 that the intensity of the 8703 cm^{-1} emission line is much less than the intensity

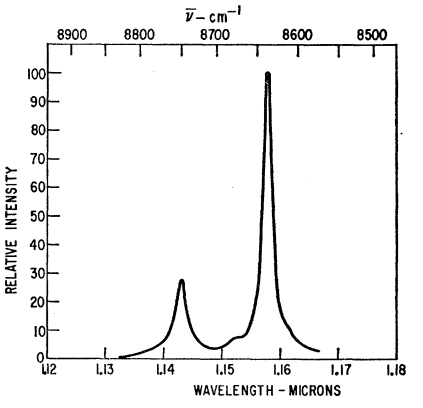

FIG. 8. Emission spectrum of $Ca_5(PO_4)_3F:MnO_4^{3-}$ at 78°K.

of the 8410 cm^{-1} emission line. Recalling the ratio of the absorption line strengths it is again seen that the 298 cm^{-1} splitting at 78°K which produces the two lines is a splitting of the excited state rather than one of the ground state. This conclusion was born out by a study of the temperature dependence of the emission line intensity ratio from 78 to 300°K. These measurements showed that the ratio grossly followed the appropriate Boltzmann factor. A detailed discussion of the positions, widths, and intensities of the sharp emission and absorption lines associated with these states will be presented separately.

In addition to these two strong lines in spodiosite, many other emission lines are seen. At 10°K essentially all of these weak lines lie at energies less than that of the intense line, e.g., less than 8410 cm^{-1} in spodiosite doped with Mn. The weak fluorescence lines are interpreted

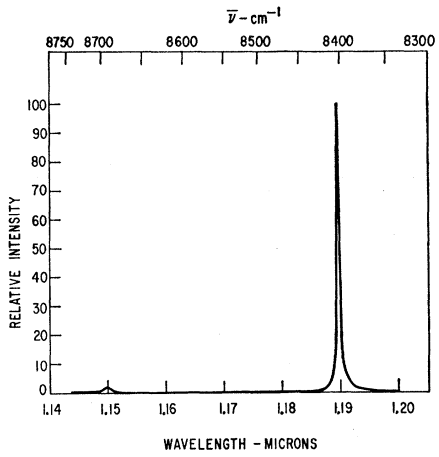

FIG. 9. Emission spectrum of $Ca_2PO_4Cl:MnO_4^{3-}$ at 78°K. Manganese concentration was 9.8×10^{18} cm^{-3}.

as arising from the excitation of vibrations of the lattice and MnO_4^{3-} ion simultaneously with the de-excitation of the electronic state of the MnO_4^{3-} ion and the emission of a photon.

Figure 10 shows the weaker fluorescence spectrum of Mn-doped spodiosite at 10°K. There is no simple variation with energy of the intensities of the many weak fluorescence peaks, and because their widths are comparable to the separations it is difficult to assign a pattern to the energies of the peaks with certainty. However, there seems to be a tendency for successive peaks to be separated by 15 cm^{-1} as is indicated by the reference marks in Fig. 10. The figure shows that about 70% of the weaker peaks are within 1 or 2 cm^{-1} of being a multiple of 15 cm^{-1} from 8410 cm^{-1}. At higher temperatures the peaks broaden and overlap until there are only smooth, structureless wings both above and below the energy of the no-phonon line, as is described below for $Ca_5(PO_4)_3Cl:Mn$.

The four most intense vibronic fluorescence transitions in spodiosite are displaced by 227, 264, 332, and

392 cm^{-1} from the 8410 cm^{-1} line. In addition to these, lines are seen at still lower energies which are separated from 8410 cm^{-1} by 555, 594, 661, 724, 788, and 833 cm^{-1}. All of the latter values are, within experimental uncertainty, various combinations of the previously mentioned four vibrational energies.

The weaker parts of the fluorescence spectrum of $Ca_5(PO_4)_3Cl$:Mn have also been investigated but in less detail. In this instance the strongest interactions occur with modes at 258, 340, and 395 cm^{-1}, both singly and in combinations. Figure 11 shows a plot of the fluorescence spectrum of a manganese-containing chlorapatite crystal at 78°K. The transitions at 8764 and 8598 cm^{-1} are believed to be pure electronic transitions and those at 8340, 8258, and 8203 cm^{-1} are those transitions accompanied by the excitation of the MnO_4^{-3} ion to vibration levels at 258, 340, and 395 cm^{-1}. The remaining significant features of Fig. 11 are the wings of the 8598 cm^{-1} line which maximize 68 cm^{-1} above and below that line and then decrease in magnitude rather slowly away from the strong line. The wing on the high-energy side of the line has the shape of the low-energy wing except that it is reversed, and its magnitude at $(h\nu-8598)$ cm^{-1} above the line is $\exp[-(h\nu-8598)$ $cm^{-1}/kT]$ times that at the corresponding energy below the line. The character of these wings, in particular their temperature dependence, is also a manifestation of the interactions of the MnO_4^{3-} ion with phonons. In this case lattice phonons of predominantly acoustic character are probably involved. The fluorescence of crystals at lower temperatures shows the high-energy wing decreasing in magnitude and the appearance of structure on the low-energy wing. Our interpretation of the weaker parts of the fluorescence spectrum will also be presented in the Discussion.

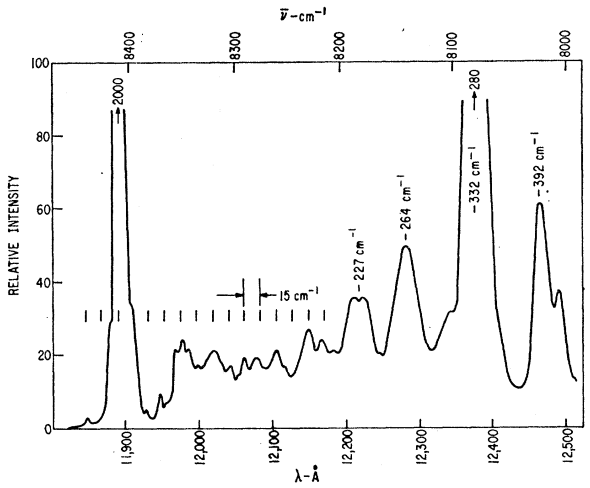

FIG. 10. Emission spectrum of $Ca_2PO_4Cl:MnO_4^{3-}$ at 10°K showing the weak fluorescence below the intense 8410 cm^{-1} line.

EXCITATION SPECTRUM

As further evidence that the broad visible absorption bands and infrared emission lines are due to the same species, the excitation spectrum of Ca_2PO_4Cl:Mn was determined. The exciting source was a tungsten lamp placed at the entrance slit of a grating monochromator. The fluorescence was filtered through a silicon wafer and a Corning C.S. 7-56 filter and detected by a 7102 photomultiplier. The excitation spectrum was found to be essentially the same as the absorption curve of the same crystal.

FLUORESCENT LIFETIMES

The fluorescence decay time of the 8410 cm^{-1} emission line of Ca_2PO_4Cl:Mn was measured using a General Radio strobotac as an exciting source. The duration of the light pulse from this source is about 3 microseconds. The fluorescence was filtered by the Jarrell-Ash monochromator, detected by a 7102 photomultiplier and the signal displayed on an oscilloscope screen. The decay time of Ca_2PO_4Cl:Mn was 0.8 msec and the other

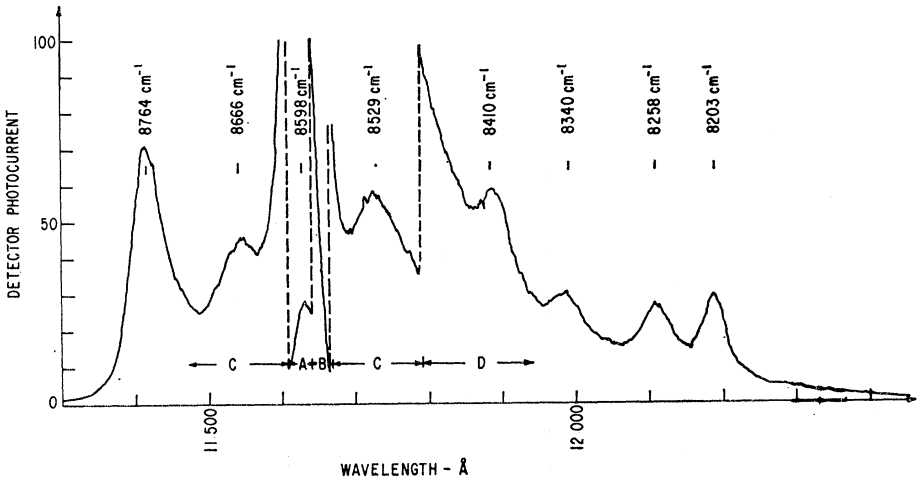

FIG. 11. Emission spectrum of $Ca_5(PO_4)_3Cl:MnO_4^{3-}$ at 78°K showing the weak fluorescence below the intense 8764 cm^{-1} line. The 8410 cm^{-1} line is believed to arise from some small contamination (probably on the surface) of these crystals by the spodiosite phase. The intensity of this line varies markedly among different crystals. Relative sensitivities: A–0.1, B–0.025, C–0.0025, D–0.001.

halophosphates studied here also all had decay times of about 1 msec. The oscillator strength of this transition in spodiosite, as determined from the absorption spectra, is about 6.5×10^{-7}. Assuming that statistical weight of the ground state is three times that of the excited state (see Discussion, Part A), we calculate a radiative lifetime of 11 msec, implying that the efficiency with which the 8410 cm^{-1} emission line is produced is about 7%.

DISCUSSION

Our results can be summarized as follows:

(1) We have prepared $Ca_5(PO_4)_3Cl$ (apatite) and Ca_2PO_4Cl (spodiosite) crystals containing Mn in an average oxidation state very close to 5+.

(2) These crystals have broad absorption bands which resemble, particularly for the apatites, the optical absorption of the MnO_4^{3-} ion in solution. A broad weak band at about 11 000 cm^{-1}, a barely resolved band at 16 700 cm^{-1}, and a narrower weak band at 13 300 cm^{-1} have been observed for the first time.

(3) In addition, in manganese-doped Ca_2PO_4Cl (spodiosite), weak narrow line absorption was found near 8410 and 8700 cm^{-1}, and a complex structured absorption between 21 500 and 25 000 cm^{-1} is present. This latter absorption spectrum we interpret as due to vibronic optical transitions.

(4) Strong infrared fluorescence near 8600 cm^{-1} was found in all the samples containing manganese. Measurements on $Ca_2PO_4Cl:MnO_4^{3-}$ indicated that there was no measurable Stoke's shift between the sharp fluorescence and absorption lines.

(5) Much weaker structured fluorescence was also found in the infrared in the vicinity of the strong sharp emission lines. These we interpret as due to excitation of various vibrations with the emission of a photon.

In Part A of this discussion we wish to consider the structure of the MnO_4^{3-} ion and the nature of its electronic states. In Part B we will discuss the spectra which we attribute to the absorption and emission of phonons simultaneous with the electronic transitions.

A. The Electronic Structure of the MnO_4^{3-} Ion

To understand the electronic spectra of Mn-doped calcium halophosphates, we must know, at least to a first approximation, the symmetry of the Mn site in the crystals. We have given chemical evidence that indicates the Mn ion has an effective ionic charge of 5+ and that it thus most probably substitutes for phosphorus, which is known to exist in $Ca_5(PO_4)_3Cl$ (apatite) as the orthophosphate ion PO_4^{3-}. The work of Lux[13] and Klemm,[14] already referred to, makes this assumption reasonable. The PO_4^{3-} ion would have the symmetry of the group T_d if it were free from external influence. Thus, it seems quite reasonable to assume that the MnO_4^{3-} ion also has approximately this symmetry in the apatite crystals. From the structure of apatite, it is known that the actual point symmetry at the phosphorous site is C_{1h}, but that the tetrahedral field of the neighboring oxygens will dominate the crystal field.

Since the structure of spodiosite (Ca_2PO_4Cl) is not known, we are less certain that the MnO_4^{3-} ion in this host will have essentially T_d symmetry. Lacking further information we will assume that it does. Considering the two possible space groups $Pca2_1$, C_{2v}^5, and $Pbcm$, D_{2h}^{11} of the orthorhombic system as determined from the observed reflections in single crystal x ray diffraction patterns,[10] the point group symmetry at the phosphorous site in Ca_2PO_4Cl is either C_1, C_2, or C_{1h}. All three of these point groups have only one dimensional representations so that all orbital degeneracy is removed.

The very strong similarity between the absorption spectra of MnO_4^{3-} ions in solution and in apatite supports our assumptions concerning the relative strengths of the tetrahedral and lower symmetry components of the field at the manganese site. The absorption spectrum of spodiosite, as shown in Fig. 3, is less similar to the solution spectrum between 4500 and 8500 Å, in that the single broad band of the latter (and apatite) is replaced by two narrower bands of comparable strength in this region. This suggests that the single broad band seen in both the apatite and solution spectra is the unresolved sum of the two bands which are more widely separated in the $Ca_2PO_4Cl:Mn$. Evidence supporting this view will be given below. That the other parts of the spectra of apatite and spodiosite, the sharp lines in the near infrared, the broad weak band at 11 000 cm^{-1} and the very strong band near 31 000 cm^{-1}, closely resemble each other, is convincing evidence that the Mn sites in the two hosts are basically the same.

Molecular orbital schemes for the tetrahedral ions MnO_4^- and CrO_4^{2-} have been described at some length by Wolfsberg and Helmholtz[4] and Ballhausen and Liehr.[5] Electron-spin-resonance measurements on single crystals containing the ions MnO_4^{2-}, MnO_4^{3-}, and FeO_4^{2-} have confirmed the molecular orbital scheme of Ballhausen and Liehr.[15] Also, this scheme leads to good agreement between calculation and measurement of the optical transition strengths for the MnO_4^- and CrO_4^{2-} ions.[5]

The ground state configuration of MnO_4^{3-}, according to Ballhausen and Liehr, is shown in Fig. 12. All of the MnO_4^{3-} orbitals up through $t_1(\pi)$ are filled (24 electrons), and the two remaining electrons half fill the $e^a(\pi)$ orbital. The configuration shown in Fig. 12 yields the three states $^3A_2$, ^1E, and $^1A_1$. Electron spin resonance measurements have shown the ground state is a triplet, hence the $^3A_2$. The crystal field theory of a d^2 ion in a tetrahedral field (T_d symmetry) predicts that the $^3A_2$ state lies lowest, followed by the ^1E and $^1A_1$.

The three lowest energy excited configurations of the

[15] A. Carrington, D. J. E. Ingram, K. A. K. Lott, D. S. Schonland, and M. C. R. Symons, Proc. Roy. Soc. (London) A254, 101 (1959).

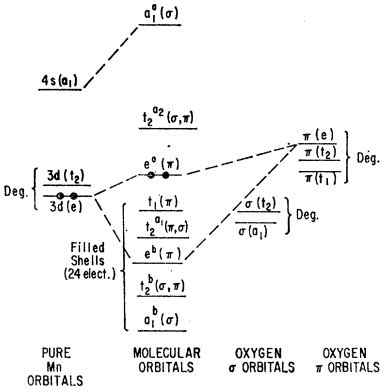

FIG. 12. Schematic molecular orbital scheme for the MnO_4^{3-} ion in the ground state configuration, according to Ballhausen and Liehr.

MnO_4^{3-} ion that can be obtained by one electron transitions from the ground-state configuration of Fig. 12 are the $t_1^6et_2$, $t_1^5e^3$, and $t_1^5e^2t_2$. The energy for the last transition should be roughly equal to the sum of the energies of the first two. We consider only those transitions which in the strong field limit correspond to one electron excitations primarily because the observed oscillator strengths are so large. As will be seen below, the strong field approximation seems appropriate for the MnO_4^{3-} ion and the absorption spectrum can be satisfactorily understood by assuming only one electron excitation.

The transitions of Ca_2PO_4Cl:Mn shown in Fig. 3 at 13 800, 17 500, and 32 400 cm^{-1} have oscillator strengths of 3.3×10^{-3}, 3.3×10^{-3}, and 2.7×10^{-2}, respectively. The magnitudes of these strengths are sufficiently large that we believe they must all be due to those electric dipole transitions which are allowed in T_d symmetry. From the $^3A_2$ ground-state, electric dipole transitions are allowed only to $^3T_1$ states. The $t_1^5e^3$ and $t_1^6et_2$ configurations each yield one $^3T_1$ state. The $t_1^5e^2t_2$ configuration yields four $^3T_1$ states, but strong transitions occur only to that $^3T_1$ state [the $t_1^5t_2(^1T_2)e^2(^3A_2):{}^3T_1$] which does not involve a spin flip. Therefore it is reasonable to conclude that each configuration is involved in one of the three absorption bands. The sum of the energies of the first two absorption bands is close to the energy of the third band.

In contrast to the spodiosite spectra, the previous studies of the absorption of MnO_4^{3-} in solution showed only two strong bands (see Fig. 2). Furthermore, on the basis of their theoretical analysis of the MnO_4^{3-} spectra, Carrington and Schonland argued that the $e\rightarrow t_2$ excitation should be considerably weaker than the $t_1\rightarrow t_2$ and $t_1\rightarrow e$ excitations and that it would appear at best as a weak band.[6] However, as will be shown in the Appendix, their argument was in error, and one cannot conclude that the strength of the $e\rightarrow t_2$ transition is weaker than the other two without a detailed calculation.

The $t_1\rightarrow e$ and $e\rightarrow t_2$ excitations should also occur strongly in the absorption bands of apatite and solution, but presumably they are somewhat closer in energy and tend to overlap into a single broad band in these cases. Our data on $Ca_5(PO_4)_3Cl$:Mn (Fig. 1) does indicate a discernible maximum at 16 700 cm^{-1} as well as the major peak at 14 800 cm^{-1} and these may be two previously unresolved excitations. Once again the sum of these two energies nearly equals the third excitation energy at 33 500 cm^{-1}.

Apparently the e orbital is displaced by about 900 cm^{-1} (6%), relative to the t_1 and t_2 orbitals in spodiosite as compared to apatite, so that the absorption bands are resolved, and apparently the change in environment is such as to make the strengths equal. The total oscillator strength of the visible absorption in apatite is 5.6×10^{-3} (compared to 1.7×10^{-2} for the MnO_4^{-3} ion in solution[6]) and this is 85% of the sum of the strengths of the two visible bands in spodiosite.

Perhaps the most interesting feature of the calcium halophosphate:MnO_4^{3-} spectra is the presence of sharp absorption and emission lines in the near infrared at 8410 and 8703 cm^{-1} in spodiosite and emission lines at 8598 and 8764 cm^{-1} in apatite. Sharp transitions occur in solids at room temperature between two states whose energy difference is insensitive to distortions of the lattice. This is usually the case only if the two states arise from the same molecular orbital configuration since the energy separations of different orbitals are quite sensitive to the positions of the various ligand ions. The sharp lines in MnO_4^{3-} must be due to transitions from the $^3A_2$ ground state to the ^1E or $^1A_1$ states, all of which arise from the e^2 configuration. In addition, we can infer from the absence of line absorption at energies less than 8400 cm^{-1} and the occurrence of fluorescence in these transitions, that the states we are concerned with are the lowest energy excited states. As mentioned previously, ligand field calculations indicate that the ^1E level is the first excited state.

The states $^3A_2$, ^1E, and $^1A_1$ are those which would occur in perfect T_d symmetry. Since the actual site symmetry is C_{1h} in apatite and either C_1, C_2, or C_{1h} in spodiosite, we are certain that all orbital degeneracy is lifted. We also expect the spin degeneracy of the $^3A_2$ state to be removed but with smaller splittings. Thus, in apatite the ^1E state splits into $^1A'$ and $^1A''$ states. We believe that the lines at 8598 and 8764 cm^{-1} in the apatite spectrum are due to the transitions $^3A''\rightarrow{}^1A'$ and $^3A''\rightarrow{}^1A''$ so that the lower symmetry components of the apatite crystal field split the E state by 166 cm^{-1}. They also split the $^3A_2$ term of T_d into three levels spaced by about 5 cm^{-1}.

The analogous splitting in spodiosite is larger, 293 cm^{-1}, if we place the states derived from the ^1E level at 8410 and 8703 cm^{-1}.

While the question of the deviation from tetrahedral symmetry is being considered, it is interesting to note that the two strong $^3T_1$ absorption bands in spodiosite at 13 800 and 17 500 cm^{-1} exhibit a definite structure

(Fig. 4). This structure we believe is also due to the lower symmetry. Maxima occur at 12 740, 13 100, and 13 790 cm^{-1} in the lower band and 17 600, 17 920, and 18 330 cm^{-1} in the upper band, so that the splittings range from 320 to 690 cm^{-1} or about the same order of magnitude of the E state splitting (293 cm^{-1}). Since the spin-orbit splitting of the et_2:$^3T_1$ state should only be about one-fourth as large as what is observed and that of the et_1:$^3T_1$ should be much smaller than that,[16] the possibility that the structure is due to that interaction can be ruled out.

The existence of the above-mentioned structure on the two absorption bands in spodiosite supports our contention that the two bands arise from different configurations instead of resulting from the splitting of the "single" band in apatite by the nontetrahedral field. In addition, the latter alternative, which would require a very marked deviation from tetrahedral symmetry in spodiosite ($V_{\text{nontet}} \approx 4000$ $cm^{-1} \approx \Delta/3$), is inconsistent with the basic similarity of the spectra in the two structures. For example, a V_{nontet} of such magnitude and any possible symmetry (E and T_2) would result in an oscillator strength for the $^3T_2$ state at 11 000 cm^{-1} comparable to that for the $^3T_1$ states (3×10^{-3}) and thus be markedly stronger than the corresponding transition in apatite. The observed f for Ca_2PO_4Cl:Mn is, however, actually slightly smaller than that for $Ca_5(PO_4)_3Cl$:Mn.

In the absence of any crystal field the ^1E state becomes the ^1D state of the free Mn^{5+} ion. This level lies at 14 500 cm^{-1} and the effect of the crystal field is to increase this energy if it does not also alter the radial part of the wave function. We conclude that the e molecular orbital wave function in MnO_4^{3-} leads to substantially smaller values of the interelectron Coulomb interaction, hence to smaller values of the B and C Racah parameters than those for the free Mn^{5+} ion. This implies that the e function is expanded in the MnO_4^{3-} ion compared to the free Mn^{5+} functions. Such an effect, although generally of smaller magnitude, has been noted in the studies of other materials. It is believed to have its origin in two different effects. In the first, the overlap of the t_1 and t_2 ligand orbitals with the $Mn^{5+}d(e)$ functions partially shields the effective Mn core charge. In the second, the expansion is due to the covalent bonding with the ligands; that is, the e orbitals contain an admixture of the ligand orbitals. That these effects can be significant in the present case is understandable in view of the large size and polarizability of the O^{2-} ion (which, in fact, does not exist as a free ion) and the large charge on the Mn^{5+} ion.

Using the prescription of Griffith[17] we calculate from the free Mn^{5+} energy levels[18] $B=1188$ cm^{-1} and $C=4879$ cm^{-1}, so $C/B=4.1$. Let us first assume, as is frequently done, that the ratio C/B is not altered by the ligand field and we place the ^1E state at 8680 cm^{-1} and the $^3T_2$ state at 11 000 cm^{-1} (the latter being the energy of the broad, weak absorption band in both apatite and spodiosite). The analytical expressions of Tanabe and Sugano[19] for the positions of these levels according to the ligand field theory give the values for B and Δ, the latter being the ligand field strength parameter. We find $B=550$ and $\Delta=11\,000$ cm^{-1}. These values predict that the $t_1^6et_2$:$^3T_1$ state lies at 16 200 cm^{-1}, which is to be compared with our previously assigned values of 14 800 or 16 700 cm^{-1} in apatite and 13 800 or 17 500 cm^{-1} in spodiosite. The agreement is fairly good even though this is probably a strongly covalent complex.

It we assume instead that $C/B=6$, we find $B=440$, $\Delta=11\,000$ cm^{-1}. These values put the $^3T_1$ state at 15 500 cm^{-1} and the $^1A_1$ state at 14 500 cm^{-1}. A narrow absorption band is seen in the apatite and solution spectra at 13 600 cm^{-1}, which is only 6% lower than the predicted position of the $^1A_1$ level.

The expressions of Tanabe and Sugano indicate that the energy of the $^1T_2$ state should be approximately equal to the sum of the energies of the ^1E and $^3T_2$ states for quite large variations in B, C, and Δ. Thus, it should lie at about 19 700 cm^{-1}. The complex absorption between 21 500 and 25 000 cm^{-1} in spodiosite may be due to transitions from the $^3A_2$ to $^1T_2$ state.

With the above ligand field parameters, we are in a position to assess the possible role of the doubly excited strong field configuration $(t_2)^2$ which arises from the free ion ^3P state and whose analogues in the weak field limit have been identified with strong absorption bands in roughly the corresponding spectral region of other materials. It is evident that if the 32 000 cm^{-1} band is to be ascribed to the $^3T_1$ state from this configuration, its oscillator strength must derive from the admixture of a $^3T_1$ state with a very large f through the Coulomb interaction. Such a state might be a charge transfer state which in this interpretation would be at an energy above 40 000 cm^{-1}. Taking the oscillator strength of the high-energy band to be one, as large as seems reasonable, and the energy separation to be 8000 cm^{-1}, the lowest possible value, we find that the matrix element connecting the $^3T_1$ states of the two configurations must be at least 1600 cm^{-1} in order to produce the observed $f=3\times10^{-2}$. The required value of 1600 cm^{-1} is comparable to the Coulomb interaction energies determined

[16] The spin-orbit splittings of the $(t_2e)^3T_1$ state are $\approx\zeta_{3d}$ and $\frac{1}{2}\zeta_{3d}$ and $\frac{1}{2}\zeta_{3d}$ and $\frac{1}{4}\zeta_{3d}$ in the weak and strong coupling field limits, respectively. Here ζ_{3d} is the $3d$ one-electron-coupling parameter as defined by Condon and Shortley and its value for the Mn^{5+} free ion is approximately 250 cm^{-1}. The contribution to the splitting from the oxygens is neglected since $\zeta_{2p}(O^-)$ is estimated to be only $\approx\frac{1}{4}\zeta_{3d}(Mn^{5+})$ and the wave function is believed to be more concentrated on the Mn ion. Recognizing that the strong field limit applies, we see that calculated splittings are too small by a factor of nearly 4. The spin-orbit splitting of the $(et_1)^3T_1$ state is even smaller since the t_1 orbital is on the O^{2-} and the matrix elements of orbital angular momentum vanishes for the e functions.

[17] J. S. Griffith, *The Theory of Transition-Metal Ions* (Cambridge University Press, Cambridge, 1961), p. 96.

[18] Charlotte E. Moore, Natl. Bur. Std. (U. S.) Circ. **467**, 41 (1952).

[19] Y. Tanabe and S. Sugano, J. Phys. Soc. Japan **9**, 753, 766 (1954).

above which related to orbitals (e and t_2) largely concentrated on the Mn and with similar radial dependences. This seems unreasonable since the B and C connecting t_2^2 configuration to the charge transfer states would be essentially overlap integrals and thus significantly smaller than those given above. Perhaps a more likely possibility for the $t_2^2:{}^3T_1$ state is that giving rise to the relatively weak structure around 23 000 cm^{-1}.

B. Vibronic Transitions

It is evident that the complex absorptions of $Ca_2PO_4Cl:Mn$ which lie between 21 500 and 25 000 cm^{-1} and the weaker parts of the fluorescence spectra, which we have seen, are due to transitions of the crystal in which both the electronic state of the MnO_4^{3-} ion and the vibrational state of the MnO_4^{3-} ion or the lattice change simultaneously. These are frequently referred to as "vibronic" transitions and have been seen in other systems but the manganese-doped halophosphates are unusual in terms of the resolution and extent of their vibronic transitions, particularly for the lower energy phonons.

The phonon energies that can be deduced from our spectra can be separated into two groups, essentially on an energy basis. In $Ca_2PO_4Cl:Mn$ (spodiosite) the first of these groups has the energies 750, 460 cm^{-1} (Fig. 5); 392, 332, 264, and 227 cm^{-1} (Fig. 10). We believe that these are energies of vibrational modes which are localized on the MnO_4^{3-} ion or the PO_4^{3-} ion.

A molecule, XY_4, having T_d symmetry has four vibrational frequencies. Two of these belong to normal modes transforming as the T_2 representation, one as the A_1 representation, and one as the E representation of the group T_d. The T_2 modes are optically active and thus appear in the infrared absorption of the PO_4^{3-} molecule ion. Infrared transmission measurements of undoped Ca_2PO_4Cl showed that the lower energy T_2 mode is split into two modes having frequencies of 532 and 595 cm^{-1}. The higher frequency T_2 modes lie between 1000 and 1100 cm^{-1}. Herzberg[20] quotes the values 515 and 1082 cm^{-1} for these PO_4^{3-} modes, indicating that the PO_4^{3-} ion is perturbed by the lattice, although not strongly. We assume, therefore, that in the crystal the PO_4^{3-} A_1 mode is approximately at the free ion value[20] of 980 cm^{-1} and similarly that the E mode is at about 363 cm^{-1}.

The A_1 mode frequency does not depend on the mass of the central ion and the ClO_4^- and SO_4^{2-} ions have this mode at 935 and 981 cm^{-1}, respectively, indicating that the force constants for all three oxyanions are equal within 10%.[20] In all three of these ions s and p orbitals are involved in the bonds. Because the MnO_4^{3-} bonds involve the more tightly bound Mn d orbitals we expect a reduction in the force constant between the central ion and the oxygens, which apparently are separated by a distance which is even larger than that in the PO_4^{3-} ion.[14] Therefore, the 750 cm^{-1} vibration which appears in our vibronic spectrum is probably either the A_1, or perhaps the T_2, mode of the MnO_4^{3-} ion. If it is the A_1 mode, as seems most probable, the force constant is reduced to about 60% of the corresponding value for the PO_4^{3-} ion. Ballhausen[21] analyzed Teltow's permanganate spectra and determined three of the four vibrational frequencies which the MnO_4^- ion has in several of its excited electronic states. These have the values 768 cm^{-1}, 302 to 325 cm^{-1}, and 255 to 270 cm^{-1}. The first of these he assigns to the A_1 mode, which is in good agreement with the frequency we have determined.

TABLE IV. Vibronic spectra of MnO_4^{3-} in Ca_2PO_4Cl.

Electronic transition	Observed energy (cm^{-1})	Identification of vibration
${}^1E \rightarrow {}^3A_2$ (Fluorescence)	227	$\nu_2(E)$ of MnO_4^{-3}
	264	$\nu_2(E)$ of MnO_4^{-3}
	332	$\nu_2(E)$ of PO_4^{-3}
	392	$\nu_2(E)$ of PO_4^{-3}
${}^3A_2 \rightarrow {}^1T_2$ (Absorption)	460	$\nu_4(T_2)$ of MnO_4^{-3}
	750	$\nu_1(A_1)$ of MnO_4^{-3}
${}^1E \rightarrow {}^3A_2$ (Fluorescence)	15	Lattice
${}^3A_2 \rightarrow {}^1T_2$ (Absorption)	30	Lattice

The 460 cm^{-1} vibration in the vibronic spectrum is about 85% of the PO_4^{3-} T_2 modes at 532 and 595 cm^{-1} so one is tempted to assign this vibration to the corresponding T_2 mode of the MnO_4^{3-} ion. Since the reduction in the force constant is less in this case, one infers that the oxygen-oxygen force constant or the "bond bending" force constant is reduced by 28% in the MnO_4^{-3} ion.

The E mode of the PO_4^{3-} ion occurs at 363 cm^{-1}.[20] The average of the 392 and 332 cm^{-1} frequencies of $Ca_2PO_4Cl:MnO_4^{3-}$ is 362 cm^{-1} and the average of the 395 and 340 cm^{-1} frequencies of $Ca_5(PO_4)_3Cl:MnO_4^{3-}$ is 367 cm^{-1}. Both averages are close to 363 cm^{-1} and this leads us to believe that these pairs of vibrations are those modes of the calcium halophosphate lattice derived from the doubly degenerate E mode of the unperturbed tetrahedral PO_4^{3-} ion. The 264 and 227 cm^{-1} vibrations may be the analogous modes of the MnO_4^{-3} ion. Table IV summarizes the identification of the observed vibrational frequencies.

To pursue the study of the vibronic transitions further it is important to consider the symmetry requirements imposed on the transitions in question. Let us first consider the infrared fluorescence vibronic spectrum. It can be shown that the interaction permitting the "strong" transitions to occur is the spin-orbit coupling and that this interaction leads to intensities of the correct mag-

[20] G. Herzberg, *Molecular Spectra and Molecular Structure, II. Infrared and Raman Spectra of Polyatomic Molecules* (D. Van Nostrand, Company, Inc., New York, 1945), Table 39, p. 167.

[21] C. J. Ballhausen, Theoret. Chim. Acta (Berl.) **1**, 285 (1963). We wish to thank C. S. Naiman for calling this point to our attention.

nitude.[22] That vibrations play a negligible role in this regard can be shown on the basis of perturbation theory since an additional factor ($<10^{-2}$) of a vibrational interaction energy divided by a large energy denominator appears in the matrix element. Thus one would expect that a strong no-phonon transition (a 0–0 transition in molecular terminology) should occur. The fact that there is no Stoke's shift between the absorption and emission lines demonstrates that this is so.

We wish to determine for the above conditions, i.e., that a transition between initial and final states of symmetries Γ_i and Γ_f, respectively, is allowed or is weakly allowed, whether a vibrational mode of symmetry Γ_v can be simultaneously excited with the electronic transition. Here we do not consider vibronic processes involving the admixture of other electronic states since these are much weaker.[23] The symmetry Γ_v will be permitted if the direct product of Γ_v and the final (or initial) state $\Gamma_v \times \Gamma_f$ ($\Gamma_v \times \Gamma_i$) contains the irreducible representation Γ_f (Γ_i). In more physical terms this says that the vibration must have a symmetry such that it can combine with the electronic state to form a resultant state with the same symmetry as that of the "pure" electronic state. We are, of course, interested in the vibrational symmetries in the T_d labeling. The Γ_f and Γ_i are clearly those for the ^1E and $^3A_2$ states despite the fact some small components of other states must be admixed into these states in order to make the transitions possible. (The electron-vibrational interaction is significant only for those components that have appreciable amplitude.) We find that in addition to the totally symmetric vibration A_1 the E mode also satisfies these conditions. As mentioned above, the modes associated with this electronic transition had been tentatively identified as the E modes on the basis of analogy with the PO_4^{3-} vibrations. The higher frequency A_1 mode has not been observed in the fluorescence.

From our study of the electronic structure we suggested that the absorption in the blue was due to the $^3A_2 \rightarrow {}^1T_2$ electronic transition, which is also forbidden in the pure tetrahedral case. We believe, on the basis of its oscillator strength, that this transition also derives its strength from the spin-orbit interaction.[24] Furthermore, since both the E and T_2 vibrations could admix T_1 component into the T_2 state to provide the strength of the transition if this were the dominant mechanism, one would expect two series of lines instead of one.

By the same considerations as above, we can see that allowed modes for this case are the A_1, E, and T_2 vibrations, which are, in fact, all the possible modes. The earlier tentative assignments of the 460 and 750 cm^{-1} vibrations as the T_2 and A_1 modes, respectively, are thus not inconsistent with symmetry requirements. Distinct peaks associated with the E mode have not been seen, but, if present, they would fall at the maximum of the continuum and perhaps be obscured.

There is a striking difference between the relatively strong coupling to the A_1 mode in the blue, as evidenced by the intensity and number of the absorption pattern replication, at intervals of the 750 cm^{-1} mode, and the weaker coupling of this vibration in the infrared as witnessed by the absence of this mode. As noted in the previous section, there is a change of configuration ($e^2 \rightarrow et_2$) associated with the transition in the blue. Since it is expected that the t_2 orbital would contain an appreciably larger amount of ligand admixture, the configuration curves for the ground and excited states should be significantly shifted and different in curvature. Concomitantly, there will be the excitation of several vibrations. In contrast, the infrared transitions involve no change in configuration, and the difference in energies of the initial and final states as a function of vibrational coordinate should be relatively constant. This reflects itself in the notable sharpness of the emission and absorption lines, as we have emphasized earlier. If the curves for the two electronic states were identical, there could be no change in phonon number with the electronic transition in the Franck-Condon approximation.

The reasons why the other mode (460 cm^{-1}) appears more weakly in the blue absorption can be understood in terms of the above picture. If this mode corresponds to a single nontotally symmetric vibration, e.g., T_2 as suggested above, it must come in through the correction to the Born-Oppenheimer approximation via the electron-vibrational interaction. As a consequence it should appear relatively weakly. Another possibility is that the 460 cm^{-1} energy corresponds to the double excitation of a nontotally-symmetric vibration, specifically that with the energy 227 cm^{-1}, since this is possible within the Franck-Condon approximation.[25] Since the change in the magnitude of the ligand field would be expected to be less for the nonsymmetric modes than for the symmetric (breathing) mode, the intensity of the vibronic lines would be low. The lack of a line at 528 cm^{-1} (i.e., two 264 cm^{-1} vibrations) tends to argue against this alternative.

---

[22] The oscillator strength arising from this mechanism would be approximately $f(^3A_2 \rightarrow {}^3T_1) V^2 [E(^1E) - E(^3A_2)] / [E(^3T_1) - E(^1E)]^3$, where V is the matrix element of the spin-orbit interaction. Taking V to be $\frac{1}{2}\sqrt{6}\zeta_{3d} \approx 300$ cm^{-1}, we calculate the oscillator strength to be $\approx 10^{-3} f(^3T_1) \approx 3 \times 10^{-6}$ which is close to the observed values of $\approx 10^{-6}$.

[23] If we view both the process considered above (direct electron-vibration coupling with the ^1E or $^3A_2$ states) and those involving the admixture of other electronic states from perturbation theory, we find that the former have matrix elements with energy denominators equal to phonon energies ($\approx$200 to 400 cm^{-1}) while the latter have denominators equal to appreciable electronic excitations ($\approx$6000 to 8000 cm^{-1}).

[24] Taking V to be $\frac{1}{4}\sqrt{6}\zeta_{3d} \approx 150$ cm^{-1}, we find the oscillator strength (see Ref. 22) to be $\approx 10^{-5}$ as is observed. On the other hand, the strength estimated on the basis of the mechanism involving a vibrational mode is lower than the above by somewhat more than a factor of 10.

[25] H. Sponer and E. Teller, Rev. Mod. Phys. **13**, 75 (1941).

If one assumes the valence bond forces model which has been reasonably successful for free molecules,[26] the four frequencies of the normal modes of a free tetrahedral molecule may be expressed in terms of two force constants and the atomic masses. Since our spectra have given us three frequencies, we may check the consistency of our assignments with the expressions for the frequencies. Using 750 cm^{-1} as the energy of the A_1 mode and 245 cm^{-1} as that of the E mode, we calculate that the two T_2 modes should have energies of 200 and 900 cm^{-1}, both values being far from the assigned energy of 460 cm^{-1}. Choosing various other assignments for two of these three frequencies does not lead to any better agreement with the third frequency. This tends to support the view that 460 cm^{-1} is not one of the fundamental frequencies of the MnO_4^{3-} ion, but rather a second harmonic. Otherwise, either at least one of our MnO_4^{3-} frequency assignments is incorrect, or the valence-bond model is inappropriate for the ion in the spodiosite lattice.

The second set of phonon frequencies appearing in our spectra includes the low energy vibrations separated by about 15 cm^{-1} in the infrared fluorescence (Fig. 10) and by 30 cm^{-1} in the visible absorption and the smooth continuum (Fig. 6). The detailed nature of these modes is quite interesting but because of our meager knowledge concerning the crystal structure and other properties of the host we can only speculate as to the nature of these vibrations.

The values 15 and 30 cm^{-1} are of the order of $\frac{1}{10}$ the energies of the modes of molecule ions having 2 to 5 nuclei. Therefore, the ratio of the force constant to reduced mass of this mode must be of the order of 100 times smaller than the same ratio for a simple molecule. The force constants of the modes we have observed in the halophosphate lattice probably are not more than two or three times smaller than the force constants of simple molecules, so the reduced mass must be 30 to 50 times larger. The crystallographic unit cell of Ca_2PO_4Cl contains 32 atoms, so a characteristic frequency of the order of 15 cm^{-1} is not unreasonable.

An attempt to relate all the peaks to multiple excitations of a single 15 cm^{-1} lattice mode would most probably fail. For, it would be difficult to reconcile the complex variation of intensities and the imperfect regularity of the spacing with this hypothesis. Furthermore, since the crystallographic unit cell is so large there will be large numbers of lattice bands extending from zero to the highest frequency "optical" mode, which probably is about 1000 cm^{-1}. It follows that one could expect a very complex density of lattice frequencies with a large number of peaks arising from critical points throughout the lattice frequency range.

In view of the anticipated complexity of the lattice mode spectrum and our lack of information about it, it is of course impossible to make a detailed interpretation of the vibronic spectra under consideration. However, the interesting general regularity might be understood in terms of a simple picture. We first consider the lattice bands $\omega(\mathbf{k})$ in an extended zone rather than in the reduced zone scheme, as is indicated schematically in Fig. 13. The bands above the true "acoustic" modes, which are mainly acoustic in character but which have some "optical" mode-like nature, are displaced consecutively by various reciprocal vectors. If the discontinuities at the zone boundaries are small, as has been found to be the case for polytypes of SiC,[27] and if the extended branches are nondispersive to a first approximation, there would occur a series of critical points more or less equally spaced in energy.

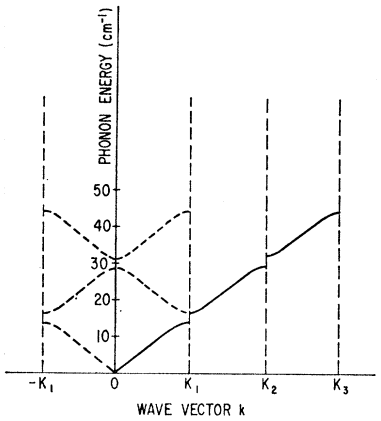

FIG. 13. Schematic lattice phonon bands in extended zone scheme. The solid lines represent one of the acoustical phonon branches in the extended zone scheme and the dotted lines this same branch in the reduced zone scheme.

We can only speculate as to the reason for the factor of 2 difference in the spacings of the vibronic bands in the infrared emission and those of the blue absorption. There is, of course, more than one branch of the type shown in Fig. 13 which could result in two constant energy differences. Also we note that the three lattice constants are in the ratios 1:1.13:1.75. If one of the electronic transitions coupled most strongly to modes propagating along the long axis while the other was more strongly coupled to waves perpendicular to the long axes, characteristic frequencies differing by about a factor of 2 might be reasonable.

Finally, it is interesting that the assignment of the 750 cm^{-1} frequency to the A_1 mode and the 460 cm^{-1} frequency to the double excitation of the E mode might be interpreted as evidence that the electronic transition responsible for the blue absorption is strongly coupled only to totally symmetric vibrational states since even orders of excitation of any mode yield totally symmetric state. Therefore, the observation of a 30 cm^{-1} spacing in the blue and 15 cm^{-1} spacing in the infrared may be consistent with this picture.

The resolution of the absorption spectrum of Fig. 6 into narrow bands and a broad band is somewhat

[26] G. Herzberg, *Molecular Spectra and Molecular Structure, II. Infrared and Raman Spectra of Polyatomic Molecules* (D. Van Nostrand Company, Inc., New York, 1945), p. 181 ff.

[27] W. J. Choyke and L. Patrick, Phys. Rev. **127**, 1868 (1962).

arbitrary. We present it as being the most obvious resolution. The smooth continuum which extends to 390 cm^{-1} resembles an acoustic phonon branch as seen in phonon-assisted transition in semiconductors. The narrow band at the end of the continuum may reflect a peaking of the density of states at a zone boundary. An alternative explanation for the continuum is that it is produced by multiple excitation of the phonon branches spaced by 30 cm^{-1}, the structure being washed out since points away from the zone boundaries may be involved in multiple phonon processes.

ACKNOWLEDGMENTS

The authors gratefully acknowledge the help of F. C. Mostek and A. M. LaTorre in making many of the measurements and in growing the crystals. The chemical analysis for Ca, Cl, F, and PO_4^{3-} was performed by the analytical group of the Lamp Metals and Components Department, Lamp Division, General Electric Company. The authors also wish to thank G. W. Ludwig for permitting us to mention his preliminary ESR data on MnO_4^{3-}, and R. K. Swank for his excitation measurements. Finally, they wish to thank F. S. Ham for several helpful discussions.

APPENDIX

Before considering the oscillator strength for the $e \rightarrow t_2$ transition, it is convenient to discuss the $t_1 \rightarrow e$ transition. We adhere to the notation of Carrington and Schonland. Using the molecular orbital for the e and t_1 states, Carrington and Schonland[6] show that the dipole matrix element for the transition is

$$a=\langle t_1, y|y|e_1, x^2-y^2\rangle=2\lambda\langle \pi y|y|d_{x^2-y^2}\rangle-\mu R/2\sqrt{3} \\ =\lambda I-\mu R/2\sqrt{3}, \quad \text{(A1)}$$

where I is an overlap integral between oxygen (O) and metal ion (M) orbitals (the so-called "charge transfer" integral), R is the OM distance, and λ and μ are the coefficients of the metal d orbital and the Oπ orbitals, respectively. From (A1) Carrington and Schonland concluded that the oscillator strength f depends separately on an overlap term and on a term varying linearly with R and that a reasonable oscillator strength could be obtained even where the overlap is small. In their numerical estimates of f for various oxyions, which included the MnO_4^{3-} ion, they in fact neglected the overlap completely.

That their conclusion about the oscillator strength is incorrect can be most readily seen by considering the determination of f in terms of the matrix elements of the momentum operator $\mathbf{p}$. Because the O orbitals for both the e and t_1 states are p functions, the matrix elements of $\mathbf{p}$ between orbitals on the same O atom vanish by the parity selection rule. The total matrix element thus consists only of overlap integrals; and, if the O-O overlap integrals are neglected compared to the O-M integrals because of the relatively large O-O interatomic distances, the matrix element is proportional to an O-M overlap integral. The momentum matrix element and hence the oscillator strength go to zero exponentially as R becomes large.

To understand how the determination of f in terms of the dipole matrix element leads to the same result it is useful to reconsider the well-known expression for f in terms of the dipole matrix elements a little more carefully than is usually done. This relation is established by making use of Ehrenfest's formula $\langle b|\mathbf{p}|a\rangle = -im(E_b-E_a)\hbar^{-1}\langle b|\mathbf{r}|a\rangle$.[28] To derive this formula it is necessary to take $\langle b|$ and $|a\rangle$ to be eigenfunctions of the Schrödinger equation, and E_b and E_a to be the corresponding eigenvalues. The connection with the above result is achieved by considering the nature of the LCAO approximate solutions. The appropriate e function for the case in hand (the e function deriving from the metal d orbital) contains an admixture of oxygen p orbital of magnitude μ which for moderately small overlap is directly proportional to O-M overlap. The total dipole matrix element is then proportional to overlap, and of course becomes negligible when the latter becomes vanishingly small. [There is another LCAO approximate e function at a different eigenvalue which consists essentially only of Oπ orbitals for small overlap (i.e., $\lambda \approx 0$ and $\mu \approx 1$). But this solution is approximately degenerate with the t_1 orbital, and the $f(t_1 \rightarrow e)$, which is proportional to $E(e)-E(t_1)$ vanishes exponentially with R as the overlap becomes small.]

We now note that the Carrington and Schonland argument purporting to show that the intensity of the $e \rightarrow t_2$ transition is rather weak was based on their assumption that the "charge transfer" integrals J and K are negligible in analogy with their erroneous conclusions regarding the $t_1 \rightarrow e$ and $t_1 \rightarrow t_2$ transitions.

[28] L. I. Schiff, *Quantum Mechanics* (McGraw-Hill Book Company, Inc., New York, 1949), p. 247.